

Suspended sediment measurements and calculation of the particle load at HPP Fieschertal

Conference Paper**Author(s):**

[Felix, David](#) ; [Albayrak, Ismail](#) ; [Abgottspon, André](#); [Boes, Robert](#) 

Publication date:

2016-11

Permanent link:

<https://doi.org/10.3929/ethz-b-000125446>

Rights / license:

[Creative Commons Attribution 3.0 Unported](#)

Originally published in:

IOP Conference Series: Earth and Environmental Science 49(12), <https://doi.org/10.1088/1755-1315/49/12/122007>

Suspended sediment measurements and calculation of the particle load at HPP Fieschertal

D Felix¹, I Albayrak¹, A Abgottspon² and R M Boes¹

¹ Laboratory of Hydraulics, Hydrology and Glaciology (VAW), ETH Zürich, Hönggerberggring 26, CH-8093 Zurich, Switzerland

² Competence Center for Fluid Mechanics and Hydro Machines (CC FMHM), Hochschule Luzern (HSLU), Technikumstrasse 21, CH-6048 Horw, Switzerland

felix@vaw.baug.ethz.ch

Abstract. In the scope of a research project on hydro-abrasive erosion of Pelton turbines, a field study was conducted at the high-head HPP Fieschertal in Valais, Switzerland. The suspended sediment mass concentration (SSC) and particle size distribution (PSD) in the penstock have been continuously measured since 2012 using a combination of six measuring techniques. The SSC was on average 0.52 g/l and rose to 50 g/l in a major flood event in July 2012. The median particle size d_{50} was usually 15 μm , rising up to 100 μm when particles previously having settled in the headwater storage tunnel were re-suspended at low water levels. The annual suspended sediment loads (SSL) varied considerably depending on flood events. Moreover, so-called particle loads (PLs) according to the relevant guideline of the International Electrotechnical Commission (IEC 62364) were calculated using four relations between particle size and the relative abrasion potential. For the investigated HPP, the time series of the SSL and the PLs had generally similar shapes over the three years. The largest differences among the PLs were observed during re-suspension events when the particles were considerably coarser than usual. Further investigations on the effects of particle sizes on hydro-abrasive erosion of splitters and cut-outs of coated Pelton turbines are recommended.

1. Introduction

At high- and medium-head hydropower plants (HPPs) operated on sediment-laden rivers, turbine parts are subject to hydro-abrasive erosion. This causes high maintenance costs, and reduces turbine efficiency, electricity generation and revenues. As a basis for adequate countermeasures and optimizations in the design, operation and maintenance of such HPPs, the knowledge on hydro-abrasive erosion and its consequences needs to be improved. To this end, the Laboratory of Hydraulics, Hydrology and Glaciology (VAW) of ETH Zürich and the Competence Center for Fluid Mechanics and Hydro Machines (CC FMHM) of Hochschule Luzern, Switzerland, initiated an interdisciplinary research project.

In this project, the sediment load, the erosion of Pelton turbine runners and the efficiency changes have been measured and analyzed since 2012 at the high-head HPP Fieschertal in Valais, Switzerland. This run-of-river HPP with a free-surface flow storage tunnel has a design discharge of 15 m³/s, a gross head of 520 m, and is equipped with two horizontal 32 MW Pelton turbines [1]. The water used in this HPP comes from a glaciated catchment and is known for high suspended sediment mass concentration (SSC) and abrasion potential.



This paper deals with the description and quantification of the suspended sediment load (*SSL*) and the so-called particle load (*PL*) at HPP Fieschertal in the years 2012 to 2014, whereas other parts of the project are treated in companion papers, e.g. [1] and [2]. The term *PL* has been introduced by IEC 62364 (2013) [3] and is explained in the present paper. After a description of the setup and the methods, selected results are presented and discussed. In particular, *SSL* and *PL* are analyzed and compared over the years and in selected events.

2. Measuring techniques, instruments and setup

The following instruments and measuring techniques were used for suspended sediment measurements:

- (1) Turbidimeters;
- (2) Laser in-situ Scattering and Transmissometry (LISST);
- (3) Vibrating tube densimetry using a Coriolis Flow and Density Meter (CFDM);
- (4) A single-frequency acoustic attenuation technique using a standard installation for acoustic discharge measurement (ADM) based on the acoustic transit time method;
- (5) Pressure-based technique, i.e. the calculation of *SSC* based on static pressure, headwater level and discharge measurements in quasi-steady state conditions;
- (6) An automatic water sampler.

The instruments (1) to (3) and (6) have been installed in the valve chamber at the top of the penstock. (1) to (3) are fed from the penstock by a sampling pipe. The measuring techniques (4) and (5) used pre-existing sensors. All instruments except the automatic water sampler are used for continuous real-time measurements of *SSC*. The automatic water sampler is used for discontinuous *SSC* reference measurements. The LISST technique additionally yields continuous real-time measurements of the particle size distribution (PSD) in the nominal range of 2 to 380 μm . Further information on the instruments and the measuring techniques as well as on the setup are given in [1] and [4].

3. Methods

3.1. Data acquisition

The outputs of the turbidimeters, the CFDM and the ADM were recorded simultaneously at 1 Hz. The LISST was programmed to perform one burst per minute. The optical instruments were cleaned every month on average. Water samples were pumped every three days or more frequently if the trigger signal, i.e. the density measured by the CFDM, exceeded certain threshold values. Furthermore, selected variables from the HPP's control system, such as headwater level, penstock discharge, pressures upstream of the turbines and electric power outputs were recorded at 1 Hz.

3.2. Laboratory analyses

SSCs were determined by gravimetric analyses of 285 bottle samples collected in the years 2012 to 2014. The density, shape and mineralogical composition of the sediment particles were investigated in the laboratory on dried residues of selected bottle samples.

3.3. Data treatment

From the 1 Hz data, minute-by-minute average values were calculated. The outputs of the turbidimeters, the CFDM, the ADM and the LISST were converted to *SSC* time series based on the gravimetrically determined *SSCs* as described in [1] and [5]. In periods of $SSC > 2 \text{ g/l}$, *SSCs* were calculated from the data of the HPP's control system using the pressure-based technique.

From the several *SSC* time series obtained from the various measuring techniques, a continuous *SSC* time series covering the years 2012 to 2014 was compiled, representing the best estimate of *SSC*. Based on data availability and investigations of the measuring uncertainties, preference was given to the *SSCs* from CFDM when the *SSC* was above 1 g/l. Otherwise, *SSCs* from LISST were taken. When no LISST data were available, *SSCs* obtained from turbidimeters or from the acoustic technique were

used. *SSCs* from the pressure-based technique were included in the best estimate *SSC* time series only during a major flood event on July 2 and 3, 2012, when the CFDM had not been installed yet.

Based on the LISST data, the best estimate *SSCs* were split-up in five particle size classes with limits of 3, 20, 50, 100, 200 and 380 μm . Such *SSCs* are also called fraction-wise *SSCs*, because particles of given size classes are also called fractions. In addition, the time series of the median particle size d_{50} was calculated from the measurements. The d_x denotes the diameter of graded particles which is exceeded by x % of the particle mass.

3.4. Calculation of suspended sediment loads

The cumulative suspended sediment load $SSL(t)$ is the suspended sediment mass transported through the penstock or through a turbine since the start time t_0 (beginning of the observation period or of a single year) until the time $t > t_0$. Q denotes the discharge (volumetric flow rate) of the water-sediment mixture. The term ' $Q_i SSC_i$ ' is the sediment transport rate (solid mass flux) which is integrated over time using equation (1). A constant time step of $\Delta t = 1$ minute was used; i denotes the time step number.

$$SSL(t) = \sum_{i=1}^{(t-t_0)/\Delta t} Q_i SSC_i \Delta t = \Delta t \sum_{i=1}^{(t-t_0)/\Delta t} Q_i SSC_i \quad \text{in [kg] or typically [t]} \quad (1)$$

3.5. Calculation of particle loads according to IEC 62364

The concept of the so-called *PL* is described in [6] and in the IEC guideline [3]. The definition of $PL(t)$ is recalled in equation (2). The dimensionless factors k_{hardness} , k_{shape} and k_{size} account for the effects of the particle hardness, shape and size, respectively, on the erosion. The *PL* reflects the erosion potential of the particles passing through a turbine as a function of time t since a certain start time t_0 . In the model described in [3], *PL* is proportional to the erosion depth. In contrast to the *SSL* (equation 1), *PL* does not depend on the discharge.

$$PL(t) = \sum_{i=1}^{(t-t_0)/\Delta t} k_{\text{hardness},i} k_{\text{shape},i} k_{\text{size},i} SSC_i \Delta t \quad \text{in [h * g/l] or [h * kg/m}^3] \quad (2)$$

The factors k_{hardness} and k_{shape} were assumed to be constant over time (properties of the catchment area). Therefore, these factors are placed in front of the sum in the rewritten equation (3). The product of $k_{\text{size},i}$ and SSC_i in equation (2) was calculated at each time step with the second sum in equation (3) based on the fraction-wise *SSCs* in five particle size classes ($j = 1$ to 5) and the factors $k_{\text{size},j}$. These factors reflect the relative erosion potential (*REP*) of the particles in each size class, as described below. The term SSC_{ij} stands for the *SSC* in the size class j during the time step number i . According to [3], SSC_{ij} were set to zero when the respective turbine was not running ($Q_{\text{Turbine}} = 0$). In the calculation of the *SSLs* and *PLs* of each turbine, it was assumed that the *SSC* in a turbine corresponds to the *SSC* measured in the penstock.

$$PL(t) = \Delta t k_{\text{hardness}} k_{\text{shape}} \sum_{i=1}^{(t-t_0)/\Delta t} \sum_{j=1}^5 k_{\text{size},j} SSC_{ij} \quad \text{in [h * g/l] or [h * kg/m}^3] \quad (3)$$

The *REP* of particles of various sizes depends on several factors such as turbine type, location inside the turbine, and size of the turbine. Four different relations between the *REP* and particle size available in the literature were used in the present study:

- 1) As a baseline case, k_{size} was set to 1, i.e. erosion would not depend on particle size (Fig. 1a).
- 2) According to Nozaki [7] and IEC [3] the *REP* increases linearly with particle size. Nozaki selected $k_{\text{size}} = 1$ at $d = 50 \mu\text{m}$. IEC suggests to take the numerical value of d_{50} in millimetres

as k_{size} , i.e. $k_{size} = 1$ at $d = 1000 \mu\text{m}$ (Fig. 1b). In the present study, the definition by IEC was adopted for the linear type of relation between REP and particle size.

- 3) According to erosion tests in the laboratory with particle-laden turbulent flow in the gap between a rotating shaft and its housing [8], the effect of particle size on erosion was found to be non-linear ([9] published in [10], Fig. 1c).
- 4) According to more recent laboratory tests on Pelton splitters [11], particles larger than approx. $100 \mu\text{m}$ cause considerably more erosion than smaller particles (Fig. 1d). This was explained by the higher inertia of the larger particles contained in the jet causing them to impinge on the splitter, whereas smaller particles follow mainly the streamlines around the splitter [11].

The factors $k_{size,j}$ listed in table 1 were determined from figure 1 as average values within each size class. Note that $k_{size,j}$ are not comparable across the various literature sources since they do not have a common basis.

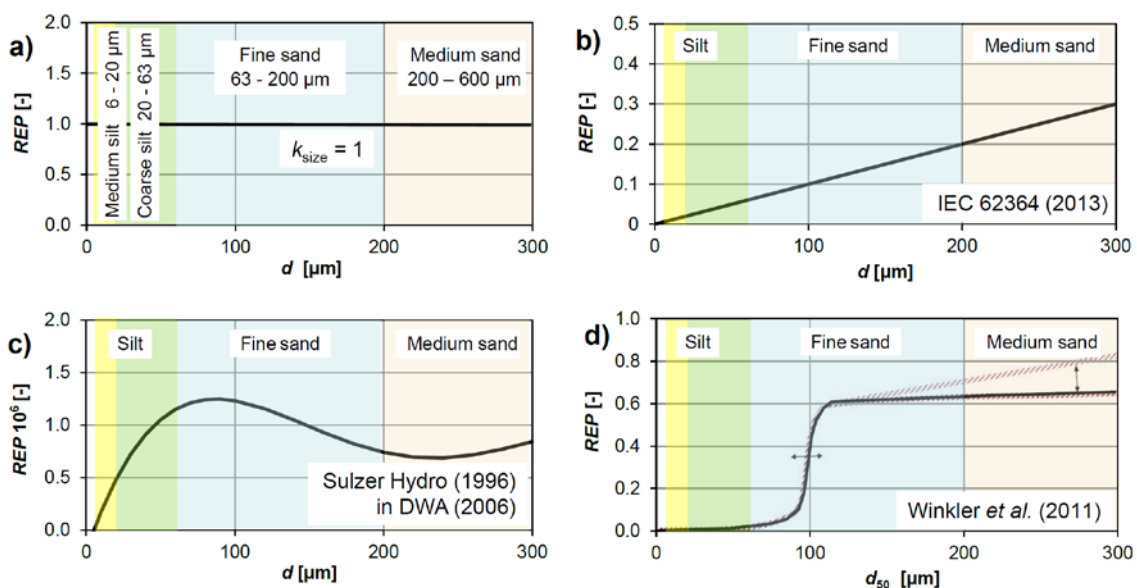


Figure 1. Relative erosion potential (REP) as a function of the particle diameter (d or d_{50}) according to four literature sources (a - d).

Table 1. REP of particles in five size classes ($k_{size,j}$) according to the relations in figure 1.

Literature source	Particle size class j [-] Range of particle diameters [μm]	$k_{size,j}$ [-]				
		1	2	3	4	5
a) Baseline case: constant		1.00	1.00	1.00	1.00	1.00
b) According to IEC 62364 (2013): linear		0.01	0.04	0.08	0.15	0.29
c) According to Sulzer Hydro (1996) / 10^6		0.21	0.79	1.20	0.99	0.81
d) According to Winkler et al. (2011)		0.01	0.02	0.08	0.60	0.70

4. Results and discussion

4.1. Density, hardness and shape of the particles

According to measurements with a Helium pycnometer on dried residues of twelve bottle samples, the solid density of the particle material is $\rho_s = 2.73 \text{ g/cm}^3$. Rietveld X-ray diffraction analyses on three samples indicated the following mineralogical composition (by mass): 30 to 40 % Quartz (Mohs hardness 7), approximately 40 % Feldspars, Epidote and Hornblende (Mohs hardness 5.5 to 7), and the rest

are softer minerals with Mohs hardness < 3 , mostly mica (Muscovite, Biotite and Chlorite). The soft particles (sheet silicates) tend to be flaky, the hard particles have generally angular shapes (Fig. 2).

These results were used to determine the values of k_{hardness} and k_{shape} based on literature. For k_{hardness} , IEC [3] suggests to take the mass fraction of the minerals which are harder than the turbine material. Because the usual base material for runners (martensitic stainless steel with 13% Cr and 4% Ni) has a Mohs hardness of 4.5, $k_{\text{hardness}} = 0.75$ was obtained. For k_{shape} , Nozaki [7] proposed values of 0.75, 1.0 and 1.25 for rounded, angular and sharp-edged particles, respectively. IEC [3] suggests to take rounded particles as the reference ($k_{\text{shape}} = 1$) and proposes $k_{\text{shape}} = 2$ for angular particles. With the hard particles being angular, k_{shape} was set to 2 according to IEC. The product of these two factors is thus:

$$k_{\text{hardness}} * k_{\text{shape}} = 0.75 * 2 = 1.5$$

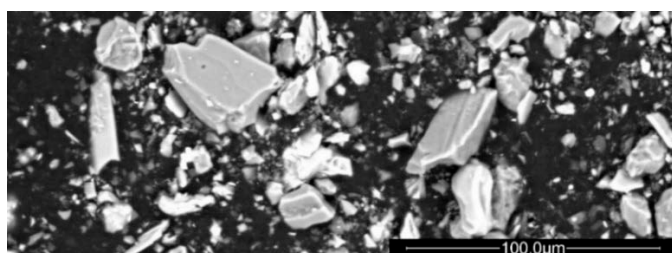


Figure 2.

Suspended sediment particles from the water sampled in the valve chamber of HPP Fieschertal (scanning electron microscope picture, ETH Zürich).

4.2. SSC, PSD and SSLs

The results of the measurements showed that the *SSC* and the *PSD* vary sometimes considerably and quickly. While the average *SSC* in the years 2012 to 2014 was 0.52 g/l, *SSC* peaks exceeding 5 g/l occurred several times a year (figure 3a). During the flood event on July 2 and 3, 2012, with an estimated return period of 20 years, the *SSC* rose up to 50 g/l.

The median particle diameter d_{50} was usually about 15 μm (in the range of medium silt) and increased occasionally to up to 100 μm (in the range of fine sand). The main reason for temporarily coarser particles in the turbine water is the operation of the headwater storage tunnel, i.e. a 2 km long free surface flow tunnel located between the intake and the inlet to the penstock: When the water level in the tunnel is high, relatively large and heavy particles settle preferentially. At low water level, the flow velocity and the bottom shear stress in the tunnel are considerably higher and previously settled particles are re-suspended [12]. The drawdowns of the water level in the storage tunnel led not only to higher d_{50} but also to higher *SSCs* (in the range of 10 g/l) when there were sediment deposits in the tunnel. A weak positive correlation between *SSC* and d_{50} was found. A reason for the low degree of correlation is the operation of the relatively small headwater storage leading to grain sorting.

The curves of the cumulative *SSL* in figure 3a show that sediment is mainly transported from mid of April to October, which is called the sediment season. The annual *SSLs* of the three years differ considerably, with the one in 2012 being the highest mainly due the major flood event in July. In all three years, 55 % of the sediment particles transported through the penstock were in the size range of fine and medium silt ($\leq 20 \mu\text{m}$), about 30 % were coarse silt (20 - 63 μm) and about 15 % were mainly fine sand (figure 3b). In 2012 the percentages of coarser particles were slightly higher than those in the other two years in which no major flood event occurred.

Figure 4b shows time series of *SSC* and cumulative *SSL* in the penstock from July 1 to 6, 2012. On July 2 and 3, the mentioned major flood event occurred; two days later a relatively high amount of sediment was re-suspended from the invert of the storage tunnel when the headwater level in the tunnel was drawn down for the first time after the flood (figure 4a). In these two events, the two highest *SSC* peaks during the three years of the study occurred and the cumulative *SSL* increased considerably in relatively short periods. Such periods are particularly important with respect to turbine wear.

During the flood event, about 17 000 t of sediment were transported through both turbines. This corresponds to 16 % of the annual *SSL* in 2012, or 33 % of the annual *SSL* in a year without any major

flood (average of 2013 and 2014). During the first and largest re-suspension event after the flood, another 4000 t of sediments passed both turbines, corresponding to 4 % of the annual SSL in 2012.

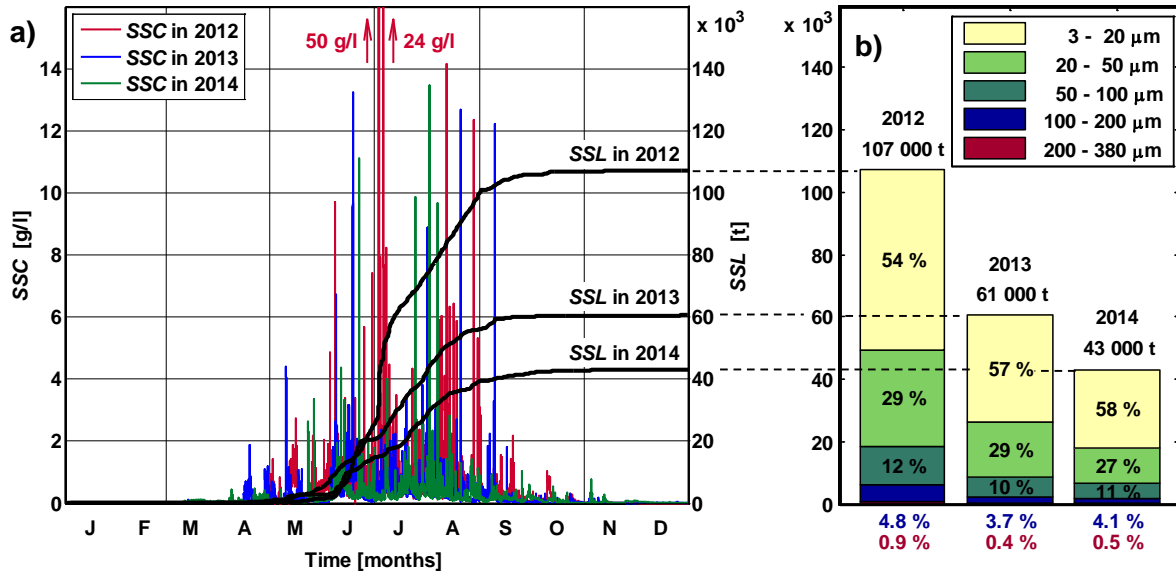


Figure 3. a) Time series of suspended sediment concentration *SSC* and cumulative sediment loads *SSL* in the penstock of HPP Fieschertal in 2012 to 2014 and b) annual *SSLs* by particle size classes.

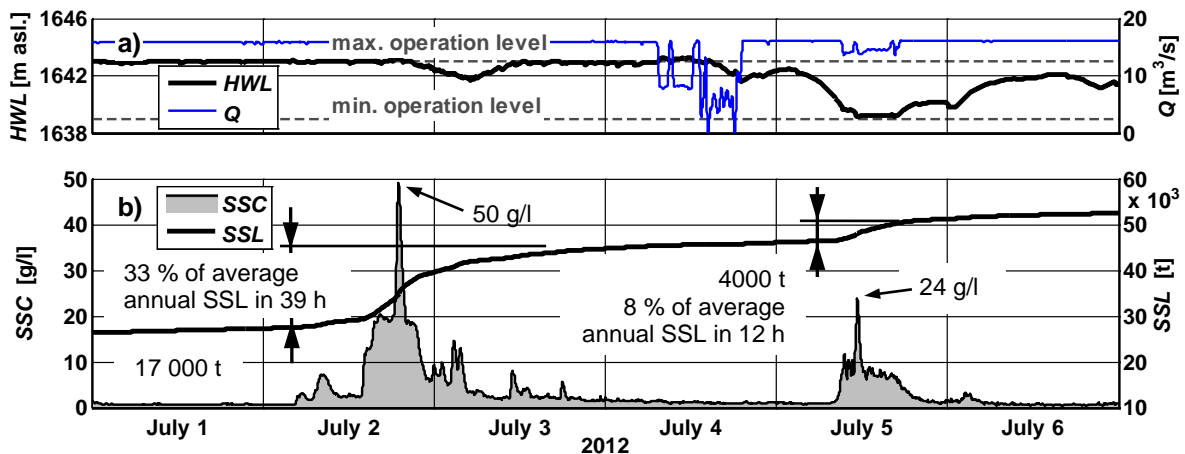


Figure 4. Time series of a) head water level *HWL* and discharge *Q* as well as b) best estimate suspended sediment concentration *SSC* and cumulative suspended sediment load *SSL* (since January 1, 2012) in the penstock at the beginning of July 2012.

Figure 5 shows the cumulative *SSL* for each turbine (called machine group, *MG*) as a function of the annual operating hours in the years 2012 to 2014. For *MG* 1, the annual *SSL* in 2012 was more than twice as high as in the other two years. The annual *SSL* of *MG* 2 in 2012 was smaller than that of *MG* 1, because *MG* 2 was out of operation from May 23 until June 22 (approx. 30 days) due to a problem at its transmission line while *MG* 1 was running almost permanently at full load. In 2013 and 2014 the annual *SSLs* were similar for both *MGs*.

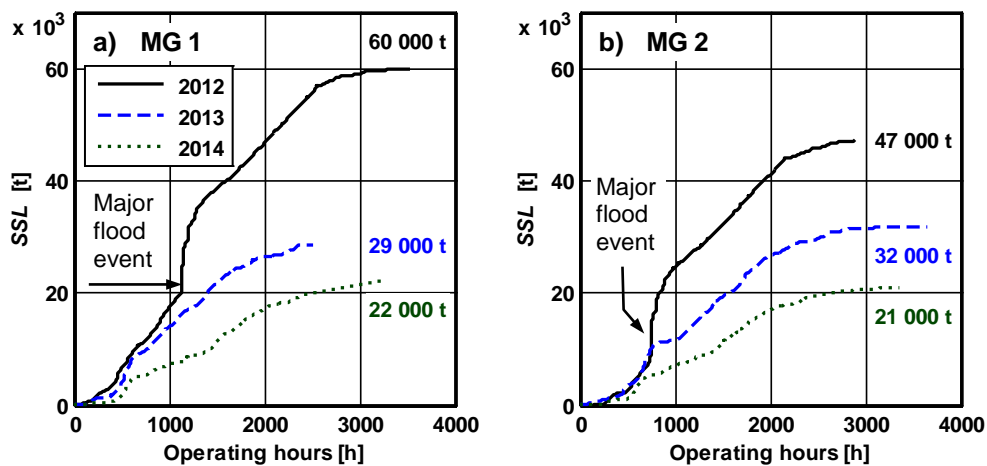


Figure 5. Suspended sediment loads SSL s for each machine group (MG) as a function of the annual operating hours in the years 2012 to 2014.

4.3. Particle loads according to IEC 62364

In figure 6, the PL with $k_{size} = 1$ and the cumulative SSL are shown for MG 1 as a function of the operating hours. The scaling of the vertical axes was adjusted to allow for a visual comparison of the two curves. The shapes of the two curves are quite similar. Comparing equations (1) and (3) with $k_{size} = 1$ yields that the curves would have exactly the same shape if either (i) the discharge Q was constant when $SSC > 0$, or (ii) if $SSC = 0$ (horizontal parts of the curves). One of the two conditions is often met due to the following reasons: (i) the HPP is generally operated at full load during the summer months when the SSC is high; and (ii) when the HPP is operated at partial load, the SSC is often low or tends to zero (in winter). The largest deviation between the two curves shown in figure 6 is observed in the second half of 2012. In the months after the flood, relatively high $SSCs$ due to re-suspension in the storage tunnel occurred while the turbines were operated at partial load.

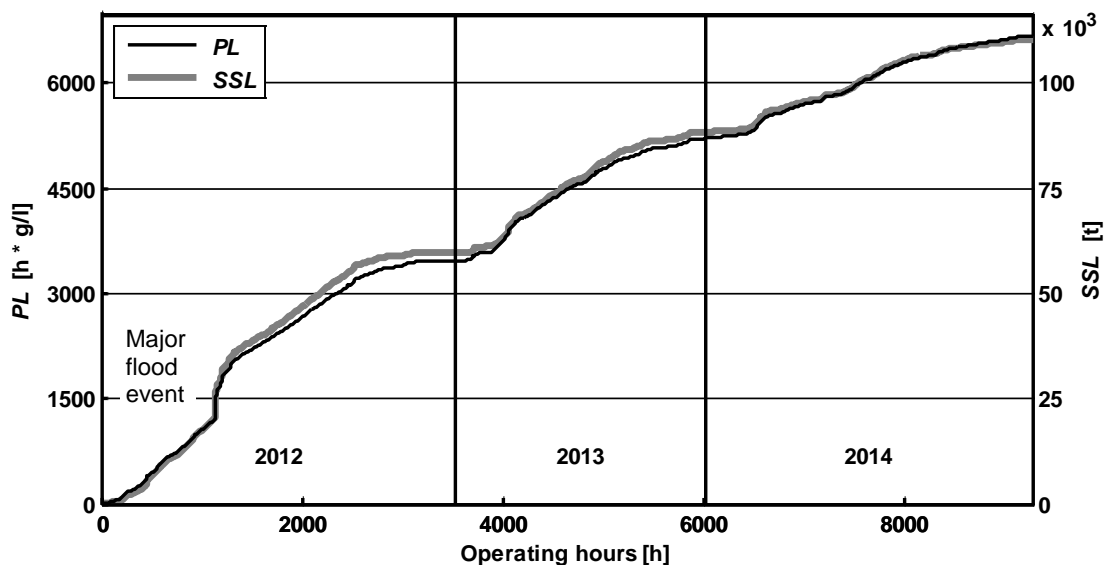


Figure 6. Particle load PL with $k_{size} = 1$ and cumulative suspended sediment load SSL of MG 1 as a function of the operating hours (since January 1, 2012).

In figure 7, the PL s of MG 1 calculated based on each of the four sets of the k_{size} -values from table 1 are shown, again as a function of the operating hours. To allow for a comparison of the shape of the curves, the PL s were normalized by their total values over the three analyzed years. As in figure 6, it is again observed that the four curves have generally quite similar shapes. The largest differences among the four curves are seen between the curve calculated with k_{size} according to Winkler et al. (2011) and the curve with $k_{size} = 1$. The main deviations between these two curves are observed (i) during and after the major flood event in 2012, (ii) in the months of late summer, and (iii) in the months of spring to early summer. The PL based on k_{size} s according to Winkler et al. (2011) was higher than the PL with $k_{size} = 1$ in the cases (i) and (ii), whereas it was the other way round in case (iii). These deviations result from the high REP of particles above some 100 μm and the low REP of the normally prevailing finer particles. In cases (i) and (ii), the particles in the turbine water were generally coarser than normally due to the flood and re-suspension events. In case (iii) the particles were generally finer than normally. This is attributed to the phenomenon that relatively fine particles, which had been eroded at the glacier bed during winter, are washed-out from the glacier by the melt-water in early summer.

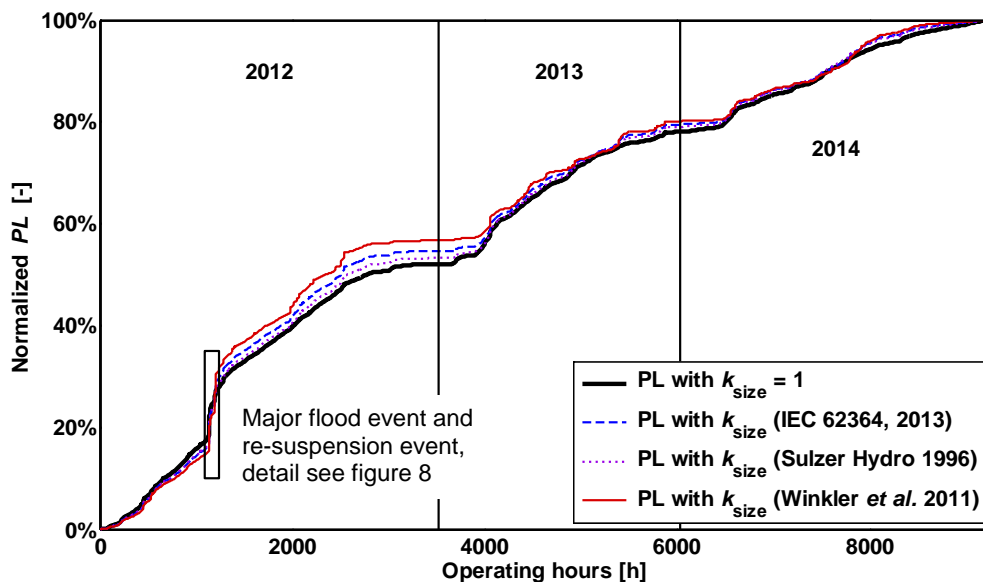


Figure 7. Normalized PL s of MG 1 calculated with four sets of k_{size} -values as a function of the operating hours from 2012 to 2014.

Figure 8 shows the time series of the normalized PL s during the first six days of July 2012. The time range is the same as in figure 4, including the major flood event and the first re-suspension event after the flood. The normalized PL calculated with $k_{size} = 1$ increased during these two events by 6 % and 2 %, respectively. The increase during the re-suspension event was thus one third of that during the flood event. With k_{size} according to Winkler et al. (2011) however, the increase in normalized PL during the re-suspension event was as high as that during the flood event (7 %). The PL calculated based on k_{size} according to Winkler et al. (2011) means that the approximately 4000 tons of mainly fine sand (mainly 63 - 200 μm) which passed the turbines during the re-suspension event (temporarily at part load) had a similar erosion potential as the considerably higher mass of finer particles (17 000 tons of mainly silt, 2 - 63 μm) during the flood event. The increases in normalized PL s during the re-suspension event calculated according to IEC (2013) and Sulzer Hydro (1996) show a higher erosion potential than with $k_{size} = 1$, too. The time series of SSC , SSL and PL s indicate that this and further re-suspension events after the flood caused considerable erosion in addition to the erosion during the flood itself.

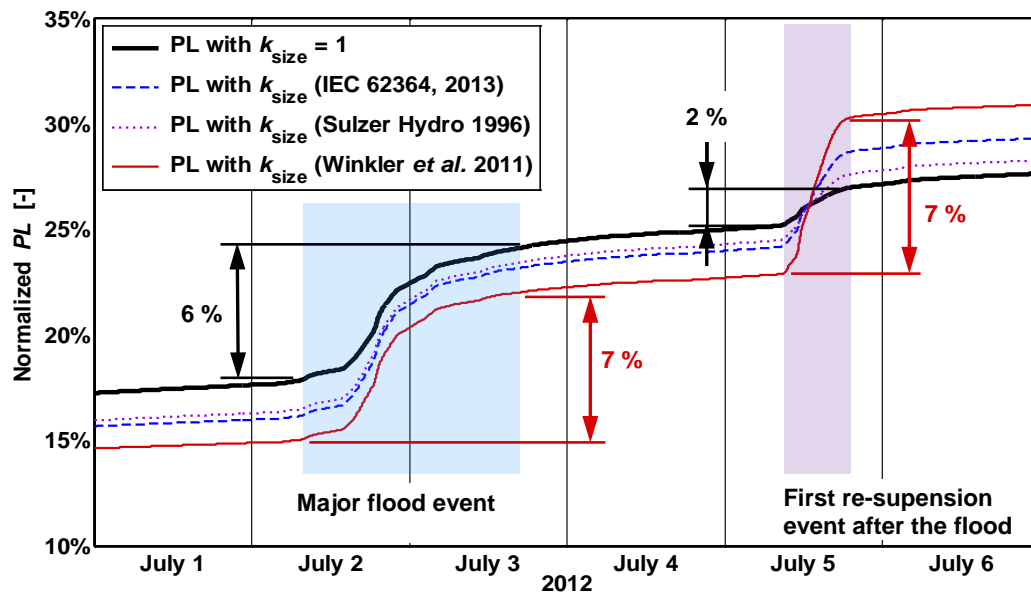


Figure 8. Detail of figure 7 in the beginning of July 2012.

5. Conclusions

SSC and PSD were measured at the waterway of the high-head HPP Fieschertal with a resolution of 1 minute during three years using an innovative combination of measuring techniques which – to the knowledge of the authors – has not been used before at any HPP.

The results of the measurements showed that SSC and PSD varied sometimes considerably, quickly and quite independently (weak correlation). In a major flood event in the beginning of July 2012, the SSC rose up to 50 g/l. The average SSC was 0.52 g/l and the d_{50} was normally about 15 μm . Coarser particles (up to 100 μm) were transported through the penstock and the turbines when the water level in the headwater storage tunnel was lowered (grain sorting due to re-suspension). High SSCs occurred due to such operational reasons or due to intense rain.

SSLs were calculated from the measured SSCs and discharges. The annual SSLs varied considerably from year to year, depending on flood events. The use of the LISST technology allowed quantifying the SSC and the SSL by size classes (fraction-wise).

In addition to the widely used SSLs, also PLs according to the recently introduced IEC guideline 62364 [3] were calculated using four sets of k_{size} -values. These factors reflect the relative erosion potential of particles of various sizes according to available literature. For the investigated HPP, the curves of the cumulative SSL and the PLs had generally quite similar shapes over three years. The PL curves deviated from the SSL curve mainly during partial load operation at relatively high SSCs. As expected from the k_{size} -factors, the largest differences among the calculated PLs were observed between k_{size} according to Winkler et al. (2011) and $k_{\text{size}} = 1$, mainly in periods when the particles were coarser than usual. The PL calculated with k_{size} according to Winkler et al. (2011) in the first re-suspension event after the major flood in 2012 was as high as during the flood event: 4000 tons of mainly fine sand (i.e. mainly in the size range of 63 to 200 μm) led to the same PL as 17 000 tons of mainly silt (i.e. mainly between 2 to 63 μm).

6. Outlook

Further investigations regarding the effect of particle size on hydro-abrasive erosion especially at splitters and cut-outs of coated Pelton turbines are recommended. Laboratory investigations offer the advantages that parameters can be varied systematically and independently, and frequent erosion mea-

measurements are possible. For feasibility reasons, however, flow conditions and geometrical relations in laboratory tests deviate from prototypes, raising questions on the transferability of laboratory results to prototype conditions (upscaling). Therefore, also further field investigations with detailed measurements at HPPs are highly recommended to enlarge the set of prototype data and to provide a basis for comparison with laboratory investigations and numerical simulations.

Acknowledgements

The support of the mentioned research project by swisselectric research, the Swiss Federal Office of Energy (SFOE), the HPP operator Gommerkraftwerke AG as well as the Swiss Competence Center for Energy Research - Supply of Electricity (SCCER-SoE) and the Research Fund of the Swiss Committee on Dams are gratefully acknowledged. Further thanks go to Endress+Hauser, Sigrist Photometers and Rittmeyer for lending measuring equipment as well as to all members of the project team for their contributions.

References

- [1] Felix D, Albayrak I, Abgottspon A and Boes R M 2016. Real-time measurements of suspended sediment concentration and particle size using five techniques. *Proc. 28th IAHR Symposium on Hydraulic Machinery and Systems*, Grenoble, France, IOP Conf. Series
- [2] Abgottspon A, Staubli T and Felix D 2016. Erosion of Pelton buckets and changes in turbine efficiency measured in the HPP Fieschertal. *Proc. 28th IAHR Symposium on Hydraulic Machinery and Systems*, Grenoble, France, IOP Conf. Series
- [3] IEC 62364 2013. Guide for dealing with hydro-abrasive erosion in Kaplan, Francis, and Pelton turbines. Edition 1.0, *International Electrotechnical Commission (IEC)*, Geneva, Switzerland
- [4] Felix D, Albayrak I, Boes R M, Abgottspon A, Deschwanden F and Gruber P 2013. Measuring Suspended Sediment: Results of the first Year of the Case Study at HPP Fieschertal in the Swiss Alps. *Proc. Hydro Conf.*, Innsbruck, Austria, paper no 18.03
- [5] Felix D, Albayrak I and Boes R M 2013. Laboratory investigation on measuring suspended sediment by portable laser diffractometer (LISST) focusing on particle shape. *Geo-marine Letters* 33(6): 485-498
- [6] Winkler K, Dekumbis R and Wedmark A 2010. Finding a way to estimate the amount of abrasion. *Proc. Hydro Conf.*, Lisbon, Portugal
- [7] Nozaki T 1990. Estimation of repair cycle of turbine due to abrasion caused by suspended sand and determination of desilting basin capacity. *Report*, Japan International Cooperation Agency, Tokyo
- [8] Grein H and Krause M 1994. Research and Prevention of Hydroabrasive Wear. *Proc. 17th IAHR Symposium on Hydraulic Machinery*, Beijing, China
- [9] Sulzer Hydro 1996. Ein semi-empirisches Abrasionsmodell zur Vorhersage von hydro-abrasivem Verschleiss an X5 CrNi 13/4 Stahl (A semi-empirical abrasion model for the prediction of hydro-abrasive wear at X5 CrNi 13/4 steel). Report STT.TB94.020 (in German)
- [10] DWA 2006 Entlandung von Stauräumen (Removal of reservoir sediments). Deutsche Vereinigung für Wasserwirtschaft, Abwasser und Abfall e.V., Hennef, Germany (in German).
- [11] Winkler K, Dekumbis R, Rentschler M, Parkinson E and Garcin H 2011. Understanding hydro-abrasive erosion. *Proc. Hydro Conf.* Prague, Czech Republic
- [12] Felix D, Albayrak I and Boes R M 2014. Variation des Feinsedimentgehalts im Triebwasser infolge Speicherstollenbewirtschaftung (Variation of suspended sediment load in turbine water due to operation of a storage tunnel). In Boes R M (ed.), *VAW-Mitteilung 227*, ETH Zurich, Switzerland: 183-193 (in German)